Supporting Information

Surface grafting polyphosphoesters on cellulose nanocrystals to improve the emulsification efficacy

Suphatra Hiranphinyophat[1], Yuta Asaumi[2], Syuji Fujii[3,4], Yasuhiko Iwasaki*[5,6]

[1]Graduate School of Science and Engineering, Kansai University, 3-3-35 Yamate-cho, Suita-shi, Osaka, 564-0836, Japan

[2]Graduate School of Engineering, Osaka Institute of Technology, 5-16-1 Omiya, Asahi-ku, Osaka 535-8585, Japan

[3]Faculty of Engineering, Osaka Institute of Technology, 5-16-1 Omiya, Asahi-ku, Osaka 535-8585, Japan

[4]Nanomaterials Microdevices Research Center, Osaka Institute of Technology, 5-16-1 Omiya, Asahi-ku, Osaka 535-8585, Japan

[5]Faculty of Chemistry, Materials and Bioengineering, Kansai University, 3-3-35 Yamate-cho, Suita-shi, Osaka, 564-0836, Japan

[6]ORDIST, Kansai University, 3-3-35 Yamate-cho, Suita-shi, Osaka, 564-0836, Japan

Tel: +81-6-6368-0090, Fax: +81-6-6368-0090, E-mail: yasu.bmt@kansai-u.ac.jp

*Corresponding author

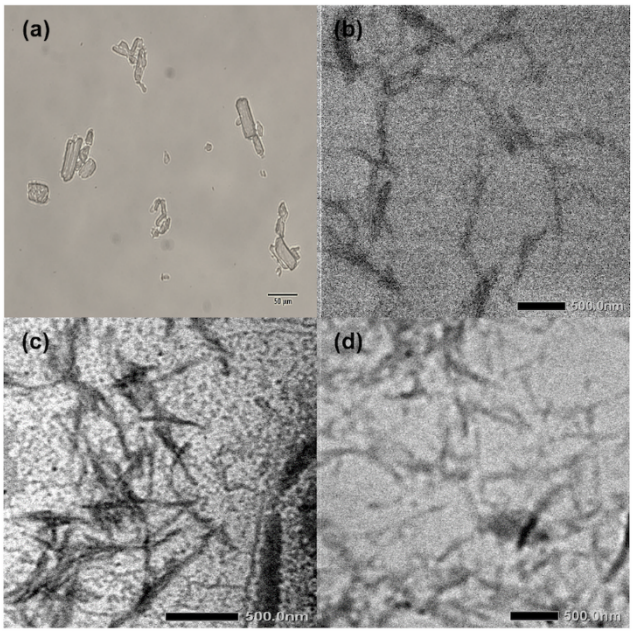

Figure S1 (a) Optical micrograph of microcrystalline cellulose (scale bar is 50 µm) and (b–d) transmission electron micrographs of cellulose nanocrystals prepared by HCl treatment for different reaction times: (b) 8, (c) 12, and (d) 16 h (scale bars are 500 nm).

Table S1 Reaction conditions and diameter sizes of cellulose nanocrystals after acid treatment.

Sample	Reaction time (h)	TEM images		DLS	
		Diameter size (nm)	Length (nm)	Diameter size (nm)	PDI
MCC	0	20 (μm)	30.4 (μm)	-	-
CNCs	8	40.6±8.7	344.3±93.2	-	-
CNCs	12	33.9±4.8	321.0±45.5	-	-
CNCs	16	22.1±7.3	250.7±62.4	-	-
CNC-*g*-PIPP	-	76.9±11.2	242.0±32.4	571.5	0.525

Table S2 Polymerization conditions of IPP in the presence of CNCs and molecular weights of free PIPP homopolymer in CNC-*g*-PIPP.

Sample ID	IPP monomer (mmol)	CNCs initiator (mmol)	Monomer conversion (%)	Grafting yield (%)	Mn[*a] (kDa)	Mn[*b] (kDa)	M_w/M_n
1	6	0.06	46.5	8.4	17.9	17.2	1.28
2	15	0.06	68.2	156.7	34.8	19.3	1.22
3	33	0.06	30.6	113.7	41.6	24.6	2.46
4	33	0.30	70.1	64.2	34.9	11.8	1.21

[a] Estimated by proton nuclear magnetic resonance.
[b] Determined by gel permeation chromatography.

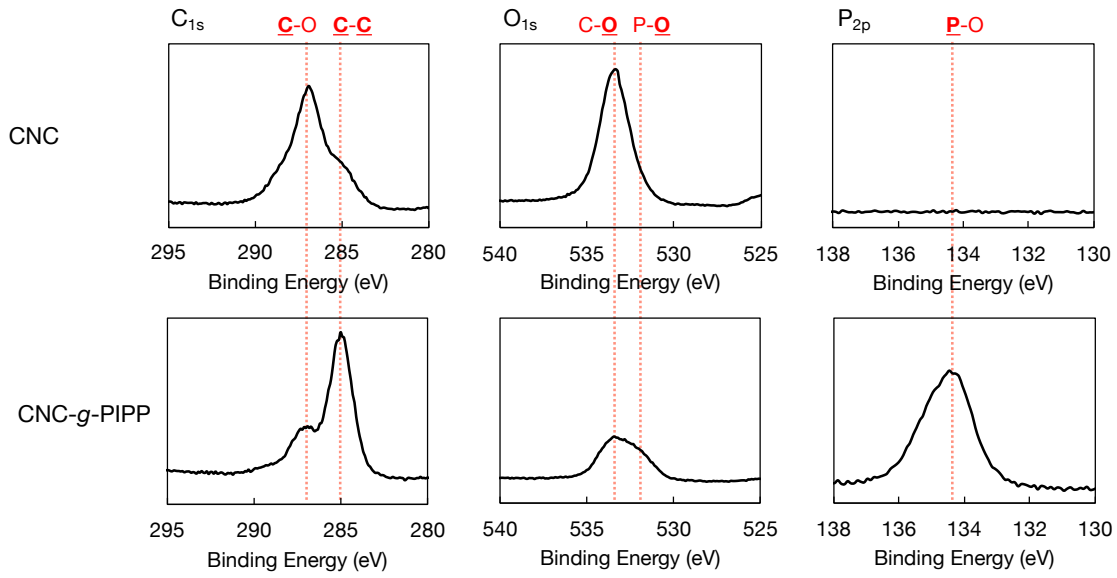

Figure S2 XPS spectra of pristine CNC and CNC-*g*-PIPP.

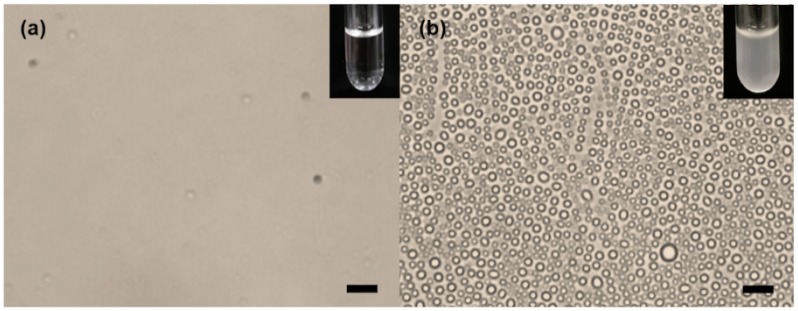

Figure S3 Phase-contrast micrographs of aqueous CNC-*g*-PIPP solutions prepared at (a) 4°C and (b) at 45°C (scale bar are 1 μm).

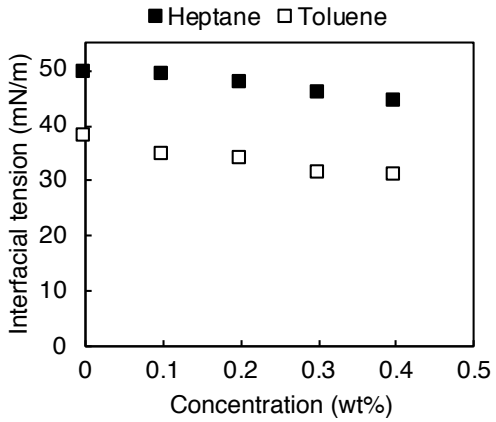

Figure S4 Interfacial tensions of toluene/water and heptane/water as functions of the concentration of unmodified CNCs at 4°C.

The percentage of CNC-*g*-PIPP nanoparticles effectively adsorbed to the oil–water interface were calculated based on the total amount of nanoparticles added by using the following equation:[1]

$$\%\text{Particles} = \frac{Total\ number\ of\ partocles\ adsorbed\ at\ droplet\ surface}{Total\ number\ of\ partles\ added} \times 100\%$$

$$= \frac{Total\ surface\ area\ of\ droplets / Total\ surface\ area\ of\ one\ particle}{Total\ volume\ of\ particles\ added / Total\ volume\ of\ one\ particle} \times 100\%$$

$$= \frac{(N_{oil} \times 4\pi R_{oil}^2) \,/\, R_{part}^2}{V_{part} \,/\, \frac{4}{3}\pi R_{part}^3} \times 100\%$$

$$= 4\pi \frac{R_{oil}^2 N_{oil}}{N_{part} R_{part}^2} \times 100\% \qquad \text{(S1)}$$

where

$$\mathrm{N_{oil}} = \frac{3V_{oil}}{4\pi R_{oil}^3} \quad \text{and} \quad \mathrm{N_{part}} = \frac{3V_{part}}{4\pi R_{part}^3}$$

where R_{oil} and R_{part} are the radii of oil droplets and CNC-*g*-PIPP particles (R_{oil} was taken to be the volume-average radius as determined by the laser diffraction and R_{part} was taken to be the particle dimension as determined by DLS measurement (Table S1)), assuming that the modified CNCs were also spherical in shape; N_{oil} and N_{part} are the numbers of oil droplets and CNC-*g*-PIPP particles (determined from the mean radius of the particles as determined by TEM images (Table S1)); and V_{oil} and V_{part} are volumes of oil and particles. However, such calculation requires an assumption to be made regarding the particle-packing efficiency at the interface. Here it is assumed that there is two-dimensional square

lateral packing, the CNC-*g*-PIPP nanoparticles are uniform, and that the sizes of the emulsion droplets and CNC-*g*-PIPP nanoparticles are negligible as compared with those of the oil droplets. It is also assumed that no nanoparticles appear in the oil phase due to the high energy barrier for the nanoparticles to enter the oil phase.

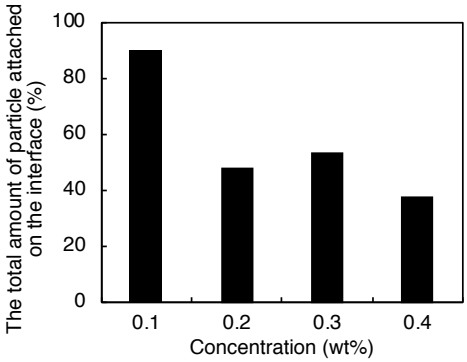

Figure S5 Percentage of CNC-*g*-PIPP nanoparticles attached to the oil–water interface as a function of the concentration.

Table S3 Microscopy images of heptane and toluene emulsions stabilized by 0.4 wt% CNC-*g*-PIPP after different storage times. Scale bars are 20 μm.

Sample/Time (min)	0	2	4	10	15
Heptane-emulsions	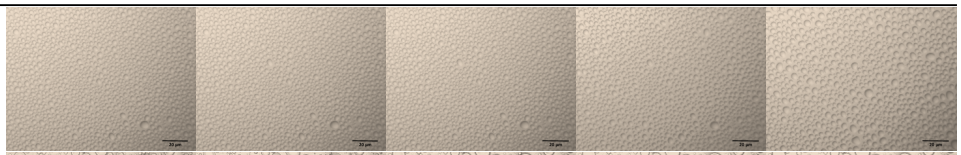				
Toluene-emulsions	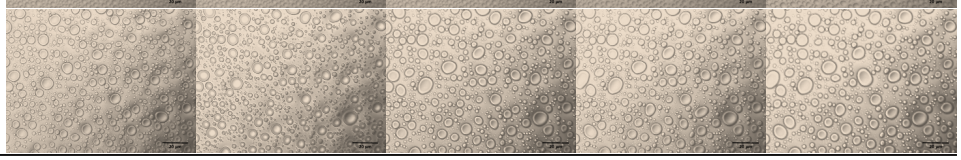				

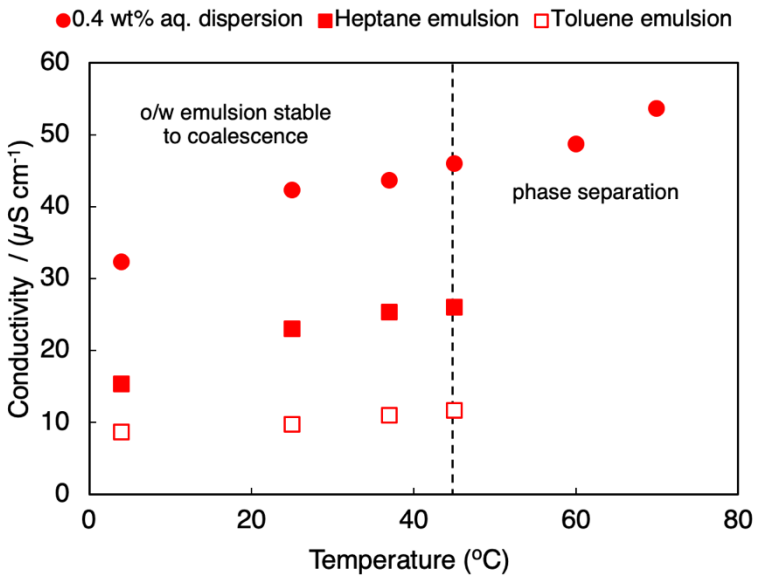

Figure S6 Conductivities of 0.4 wt% CNC-*g*-PIPP aqueous dispersions and O/W emulsions prepared with different oils (heptane or toluene) as a function of temperature.

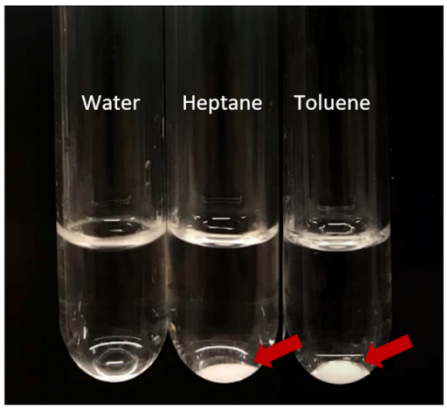

Figure S7 Pendant drop of emulsions in distilled water, heptane, and toluene stabilized by 0.4 wt% CNC-*g*-PIPP.

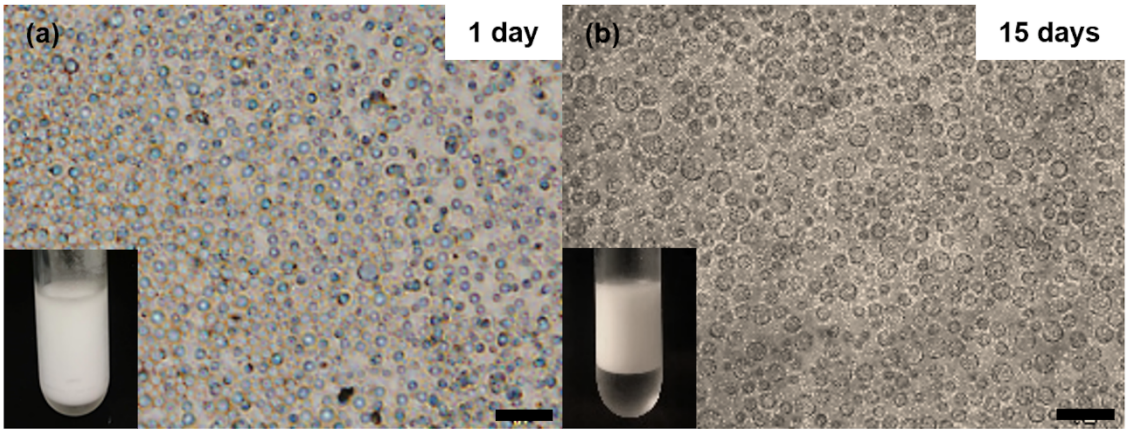

Figure S8 Optical microscopy images of emulsions prepared with 0.4 wt% CNC-*g*-PIPP after storage for (a) one day and (b) 15 days. Scale bars are 20 µm.

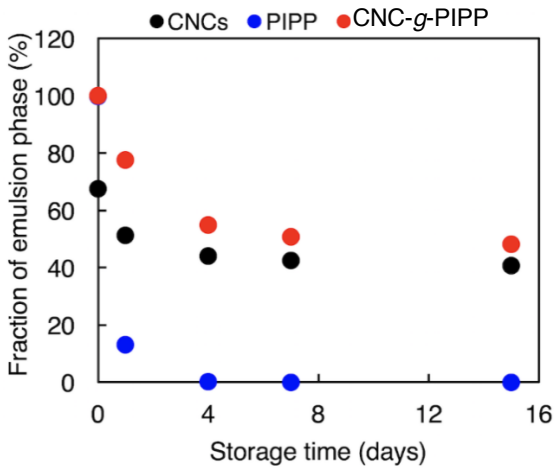

Figure S9 Proportions of the oil-in-water emulsion phase in samples prepared with 0.4 wt% CNCs, PIPP, and CNC-*g*-PIPP as functions of storage time.

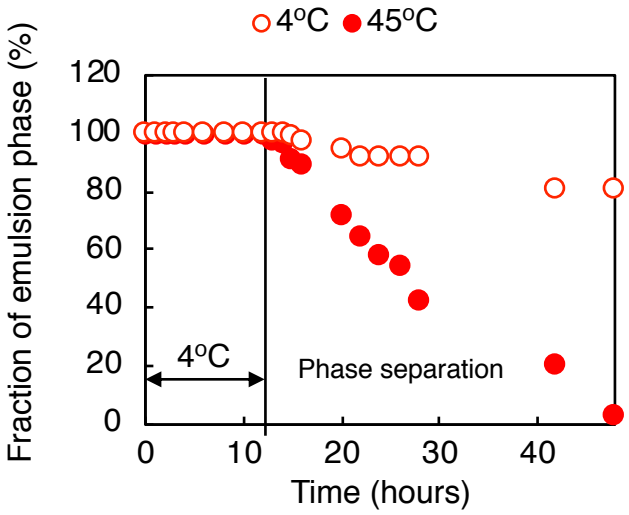

Figure S10 Creaming profile fraction of heptane in water in a Pickering emulsion stabilized with 0.4 wt% CNC-*g*-PIPP at temperatures of 4°C and 45°C.

Table S4 Partitioning behavior of modified CNCs after demulsification at different temperatures.

Temp (°C)	Phase	Total weight of sample (g)	Weight of sample in each oil phase (g)	% Partition
4	oil	0.015	0.00037	2.5
	water		0.01428	97.5
45	oil	0.015	0.01097	57.7
	water		0.00811	42.3

Reference

(1) Fujii, S.; Aichi, A.; Muraoka, M.; Kishimoto, N.; Iwahori, K.; Nakamura, Y.; Yamashita, I. Ferritin as a bionano-particulate emulsifier. *J. Colloid Interface Sci.* **2009**, 338, 222-228.